Physicochem. Probl. Miner. Process., 62(1), 2026, 216341

http://www.journalssystem.com/ppmp

Physicochemical Problems of Mineral Processing

ISSN 1643-1049

Competitive adsorption processes in mixed CTAB–alcohol systems at the surface of a liquid silver amalgam electrode (R-AgLAFE)

Alicja Pawlak [1], Agnieszka Nosal-Wiercińska [1], Mariusz Grochowski [1], Teresa Urban [2], Anna Szabelska [3]

[1] Department of Analytical Chemistry, Institute of Chemical Sciences, Faculty of Chemistry, Maria Curie-Sklodowska University; Maria Curie-Sklodowska Sq. 3. 20-031 Lublin, Poland.

[2] Department of Radiochemistry and Colloid Chemistry, Faculty of Chemistry, Maria Curie-Sklodowska University, M. Curie-Sklodowska Sq. 3, 20-031, Lublin, Poland.

[3] Department of Prosthetic Dentistry, Medical University in Lublin, Karmelicka Str. 7, 20-093 Lublin, Poland.

Corresponding author: alicja.pawlak@mail.umcs.pl, alapawlak123@interia.eu

Abstract: The study investigates adsorption processes occurring at the surface of a cyclically renewable liquid silver amalgam film electrode (R-AgLAFE) in mixed aqueous/organic solutions of supporting electrolytes (SEs) containing low-molecular-weight alcohols (methanol, ethanol, 1-propanol) and the cationic surfactant cetyltrimethylammonium bromide (CTAB). The work involved analysing competitive adsorption phenomena in systems with different liquid-phase compositions (in the absence and presence of $25\%_{(v/v)}$ and $50\%_{(v/v)}$ alcohol) and assessing their effects on the structure and properties of the electrical double layer (EDL). It was found that the adsorption of CTAB and alcohols is competitive, and its intensity depends on both the type and concentration of the alcohol. The most pronounced effects occurred in the presence of 1-propanol, highlighting the roles of hydrophobic interactions and changes in the medium's dielectric properties. The results provide new insights into adsorption mechanisms in aqueous/organic systems.

Keywords: CTAB, differential capacitance, liquid silver amalgam electrode (R-AgLAFE), competitive adsorption, potential of zero charge, surfactant-solvent interaction

1. Introduction

The significance of adsorption is particularly evident in the practical applications of electrochemistry, ranging from highly sensitive analytical systems to broader areas such as electrocatalysis and energy storage. A common approach in electrochemical research involves altering both the electrode surface (Švancara, Sýs, 2023) and the composition of the liquid phase. Typical modifiers used include organic solvents (Gu et al., 2022; Nieszporek, 2013), electroactive monomers like guaiacol (Kiss et al., 2025), and surfactants (Chibowski, Wiśniewska, 2021; Zhang et al., 2015). In some systems, adsorption phenomena coexist with effects explained by the cap-pair rule, which suggests donor–acceptor interactions between the functional groups of organic molecules and depolariser species (Martyna, Nosal-Wiercińska, Gołębiowska, 2022; Sykut et al., 1978).

As a result of adsorption in the interfacial region, several physicochemical parameters change, such as the potential of zero charge (E_z), the differential capacitance of the electrical double layer (EDL), the charge-transfer resistance (R_{ct}), and the surface tension at the potential of zero charge (γ_z). Studies examining the effect of surfactants on the electroreduction of various depolarisers on metallic electrodes (mercury, gold, amalgam) and on carbon-based electrodes, which have recently gained attention for ecological and practical reasons (Fic, Lota, Frąckowiak, 2012; Sawamoto, 2003), have confirmed these changes. For example, the adsorption of 1-decanesulfonate anions in perchlorate(VII) solutions caused noticeable shifts in E_z and variations in EDL capacitance, showing specific adsorption interactions with the mercury electrode surface (Gugała-Fekner, Nieszporek, and Sieńko, 2015). In contrast, electrochemical impedance spectroscopy (EIS) results of aluminium electrodes in mixed aqueous–

DOI: 10.37190/ppmp/216341

organic solutions containing 1-propanol demonstrated that water molecules tend to adsorb at the electrode–solution interface. The nearly constant differential capacitance of the EDL, regardless of alcohol volume fraction (at a fixed $NaClO_4$ concentration), indicates that 1-propanol affects the interfacial structure mainly indirectly, by changing the medium's dielectric properties and the solvation network (Iwasaki, Kimura, Uematsu, 2023). However, these conclusions shouldn't be generalised without critical evaluation, as literature also reports that the impact of low-molecular-weight alcohols on the EDL structure varies significantly and depends on multiple factors, including the type of electrode, solvent, and additional solutes (Moncelli, Foresti, Guidelli, 1990; Pikma et al., 2023).

For example, in systems employing platinum or carbon electrodes, shifts in the potential of zero charge (E_z) and noticeable changes in EDL capacitance have been observed when alcohols are present. These are attributed to their specific adsorption or coadsorption with electrolyte ions (Iwasaki, Kimura, Uematsu, 2023; Kusu, Takamura, Watanabe, 1993; Breiter, 1962). These observations indicate that interactions in aqueous–organic mixtures do not follow a universal pattern but rather result from a balance of competing effects.

Despite the rapid growth of research on electrochemical systems with organic solvents and surface-active modifiers, most existing data focus on crystalline noble-metal or carbon-based electrodes (Zhao et al., 2024 Pikma et al., 2023). In contrast, there are few studies examining the effects of alcohols and surfactants on the structure and properties of the EDL at amalgam electrodes, whose unique surface features, due to the presence of a liquid metal alloy, may lead to different adsorption mechanisms. Therefore, the aim of this study was to investigate competitive adsorption processes between CTAB and low-molecular-weight alcohols (methanol, ethanol and 1-propanol) at the surface of a cyclically renewable liquid silver amalgam electrode (R-AgLAFE). It was assumed that alcohols compete with CTAB for adsorption sites, and that the extent of this effect increases with alcohol chain length and volume fraction.

2. Materials and methods

2.1. The composition of the tested solutions

As the supporting electrolytes (SEs), aqueous solutions containing 0.5 mol·dm^{-3} sodium chlorate(VII) ($NaClO_4$, Fluka, ≥98.0%) and 0.5 mol·dm^{-3} chloric(VII) acid ($HClO_4$, Chempur, 70%, analytical grade) were used. To investigate the effect of the type and proportion of low-molecular-weight alcohol, solutions of the same basic electrolyte system were prepared in various mixed water–alcohol solvent systems (MeOH, EtOH, 1-PrOH; POCh, analytical grade), in which water was partially replaced with the corresponding alcohol in 25%$_{(v/v)}$ or 50%$_{(v/v)}$. All solutions were supplemented with the cationic surfactant cetyltrimethylammonium bromide (CTAB; $C_{19}H_{42}BrN$) in the concentration range of 5·10^{-5} - 3·10^{-3}mol·dm^{-3}.

For clarity, the tested solutions were designated by symbols A–G:

- System A: 0.5 mol·dm^{-3} $NaClO_4$ + 0.5 mol·dm^{-3} $HClO_4$ in water (basic solution, without alcohol) + CTAB;
- System B: 0.5 mol·dm^{-3} $NaClO_4$ + 0.5 mol·dm^{-3} $HClO_4$ in the water–MeOH system (25%$_{(v/v)}$ MeOH) + CTAB;
- System C: 0.5 mol·dm^{-3} $NaClO_4$ + 0.5 mol·dm^{-3} $HClO_4$ in the water–MeOH system (50%$_{(v/v)}$ MeOH) + CTAB;
- System D: 0.5 mol·dm^{-3} $NaClO_4$ + 0.5 mol·dm^{-3} $HClO_4$ in the water–EtOH system (25%$_{(v/v)}$ EtOH) + CTAB;
- System E: 0.5 mol·dm^{-3} $NaClO_4$ + 0.5 mol·dm^{-3} $HClO_4$ in the water–EtOH system (50%$_{(v/v)}$ EtOH) + CTAB;
- System F: 0.5 mol·dm^{-3} $NaClO_4$ + 0.5 mol·dm^{-3} $HClO_4$ in the water–1-PrOH system (25%$_{(v/v)}$ 1-PrOH) + CTAB;
- System G: 0.5 mol·dm^{-3} $NaClO_4$ + 0.5 mol·dm^{-3} $HClO_4$ in the water–1-PrOH system (50%$_{(v/v)}$ 1-PrOH) + CTAB.

2.2. Differential capacity measurements

Differential capacity measurements were performed using a μAutolab type III electrochemical analyser equipped with GpES software version 4.9 (EcoChemie B.V., Utrecht, The Netherlands) and a programmable electrode stand M165D (mtmanko, Kraków, Poland). All experiments were carried out in a three-electrode cell comprising:

- the working electrode – a cyclically renewable liquid silver amalgam film electrode (R-AgLAFE) (Nosal-Wiercińska et al., 2021) with an active surface area of 0.19822 cm^2;
- the reference electrode – a silver/silver chloride (Ag/AgCl) electrode in 3 $mol \cdot dm^{-3}$ KCl;
- and the auxiliary electrode – a platinum spiral.

All measurements were performed at a constant temperature of 25 ◦C, recording the dependence of the electrical double layer (EDL) capacitance at the R-AgLAFE/electrolyte interface over the full range of electrode polarisation. Differential capacity curves determined within the frequency range 200–1000 Hz were extrapolated to zero frequency, thereby eliminating the dispersive component and enabling the determination of parameters corresponding to the stabilised EDL structure (Lasia, 2014; Pajkossy, 2005). This procedure enabled the distinction between variations arising from the reorganisation of the electrical double layer and purely dynamic effects associated with mass transport and changes in solution resistance (Lasia, 2014).

2.3. Determination of zero charge potential and surface tension

The potential of zero charge (E_z) was determined using a streaming electrode with an accuracy of 0.1 mV. The surface tension at the potential of zero charge (γ_z) (with an accuracy of ±0.2 $mN \cdot m^{-1}$) was measured by the maximum bubble pressure method, originally developed by Schiffrin (Schriffrin, 1969) and and later applied in electrochemical studies by Nosal-Wiercińska (2010) (Nosal-Wiercińska, 2010). The obtained E_z and γ_z values provided the basis for evaluating the influence of the investigated surfactants and organic solvents on the electrostatic and structural properties of the electrical double layer (EDL). A similar procedure has been successfully applied in several studies, for example, in assessing the effect of nicotinamide adsorption at the Hg/solution interface on the electroreduction of Zn^{2+} ions (Nieszporek, 2020).

The cell constant (K_{cell}) of the electrochemical vessel was determined using a capillary electrometer and standard electrolyte solutions of KCl, NaCl, and KNO_3. The measurement was carried out by recording the height of the mercury column (h_z) corresponding to the potential of zero charge (E_z) in each standard solution. The obtained value of $K_{cell} = 8.62$ was used exclusively for calculating the surface tension at the potential of zero charge (γ_z) for the investigated systems. The use of simple electrolyte solutions with well-characterised properties as standard systems enabled precise determination of K_{cell}. It ensured comparability of results in subsequent measurements.

2.4. Determination of the critical micelle concentration (CMC)

The critical micelle concentration (CMC) of the investigated surfactants in the applied aqueous-organic systems was determined using the viscosimetric method with a CVO 50 rotational rheometer (Bohlin Instruments) coupled to a computer and an RTE 111M thermostat (NesLab). For selected systems containing both the surfactant and the organic solvent (methanol, ethanol or 1-propanol), the threshold concentration at which molecular self-assembly into micelles occurs was determined (Bhattarai, 2015). This parameter plays a key role in the present study, as it defines the point at which the dominant mechanism of surfactant interaction with the R-AgLAFE surface may change, from adsorption of individual molecules to potential deposition of micellar structures. The determination of the CMC, therefore, enabled assessment of the extent to which modification of the liquid-phase composition influences the organisation of the surfactant in the near-electrode region. Each measurement was performed in triplicate, and the reported CMC values correspond to mean values with an estimated experimental uncertainty of ± $0.15 \cdot 10^{-4}$ $mol \cdot dm^{-3}$.

3. Results and discussion

3.1. Differential capacity measurements

Comparison of the differential capacitance curves (Fig. 1) obtained for solutions containing CTAB with that of the basic electrolyte alone allows two characteristic potential regions to be distinguished: E < –0.3 V and E < –1.35 V. In the first region, an increase in differential capacitance is observed, accompanied by the appearance of CTAB adsorption peaks, whose heights increase markedly with increasing surfactant concentration. The potentials of these peaks shift towards more negative values.

The second region (Fig.1) corresponds to desorption peaks that systematically decrease in intensity while maintaining their positions up to a CTAB concentration of $8{\cdot}10^{-4}$ mol·dm^{-3}. Above this concentration (corresponding to the critical micelle concentration, CMC), a sharp increase in peak heights is observed, accompanied by a shift in their potentials. This behaviour suggests a reorganisation of the surfactant within the adsorbed layer, indicative of the formation of hemimicelles: surface aggregates representing a transitional form between the adsorbed monolayer and micelles in solution (Paria, Khilar, 2004).

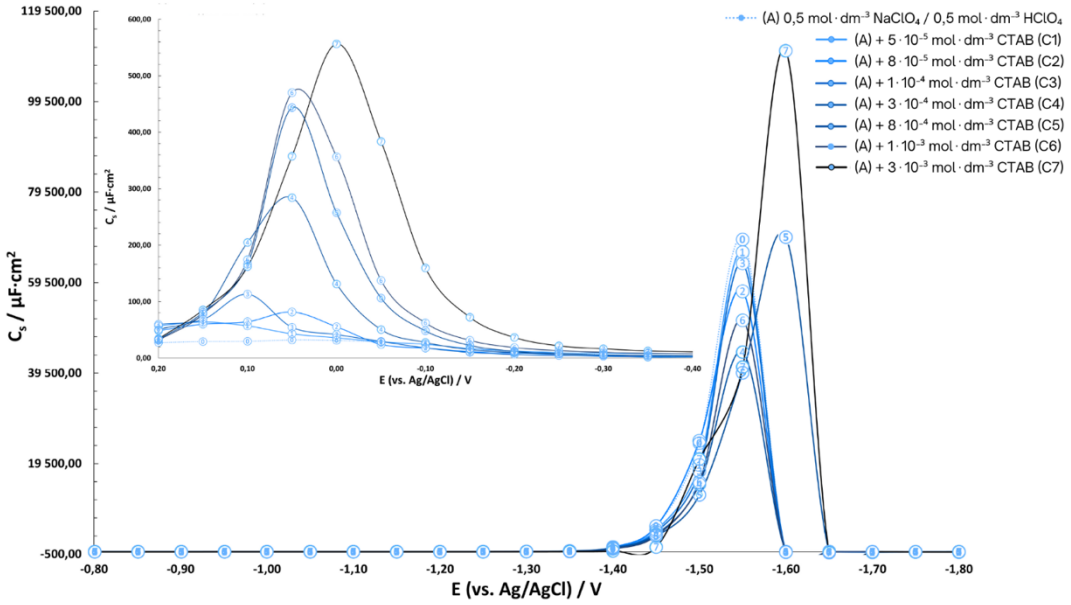

Fig. 1. Differential capacitance curves for system A: 0.5 mol·dm^{-3} $NaClO_4$ + 0.5 mol·dm^{-3} $HClO_4$ and in the presence of CTAB ($5.0{\cdot}10^{-5}$-$3.0{\cdot}10^{-3}$ mol·dm^{-3})

Figs. 2–4 present the differential capacitance curves obtained for solutions containing a fixed methanol concentration (25%$_{(v/v)}$) and varying CTAB concentrations. Comparison of these dependencies indicates that the introduction of CTAB into the basic electrolyte solution (chlorate(VII) + 25%$_{(v/v)}$ alcohol) increases the differential capacitance, as evidenced by the appearance of an adsorption peak and a characteristic desorption peak of CTAB. Both peaks increase in height with increasing CTAB concentration, while the adsorption peaks exhibit a noticeable shift towards more negative potentials. It should be noted, however, that the capacitance curves show a distinctly altered shape in the potential range –0.85 to –1.3 V (Figs. 2–3) compared with those recorded for the chlorate(VII)/CTAB system (Fig. 1). Additional peaks appear, which may indicate a reorganisation of the EDL structure due to coadsorption of CTAB and methanol. It should be emphasised that CTAB adsorbs chemically, whereas methanol adsorbs physically (specifically) (Sawamoto, 2003; Yáñez, Gutiérrez, Ureta-Zañartu, 2003). Methanol competes with CTAB for adsorption sites on the electrode surface; however, CTAB clearly dominates in forming mixed adsorbed layers. Nevertheless, the formation of hemimicelles or micelles (CMC ≈ $8{\cdot}10^{-4}$ mol·dm^{-3}) and their mutual interactions with alcohol molecules cannot be excluded, as this may lead to the development of more or less compact structures within the adsorbed layer (Bhattarai, 2015).

The differential capacitance curves recorded for solutions containing a constant alcohol concentration (50%$_{(v/v)}$ methanol) and increasing concentrations of CTAB are shown in Figures 5 and 6. The observed features of the curves indicate physical adsorption of aliphatic alcohols, with distinct adsorption and desorption peaks and variations, including a peak in the region of strong adsorption (approximately -0.4 V). The introduction of CTAB into this system, and the subsequent increase in its concentration, result in a decrease in the intensity of this peak (around -0.4 V), whereas the adsorption-desorption peaks increase in height in a typical manner and exhibit slight shifts in their potential positions. Such behaviour indicates the dominance of CTAB adsorption within the mixed adsorbed layer (Gisbert-González et al., 2023; Knag, Sjöblom, Gulbrandsen, 2005). A pronounced increase in

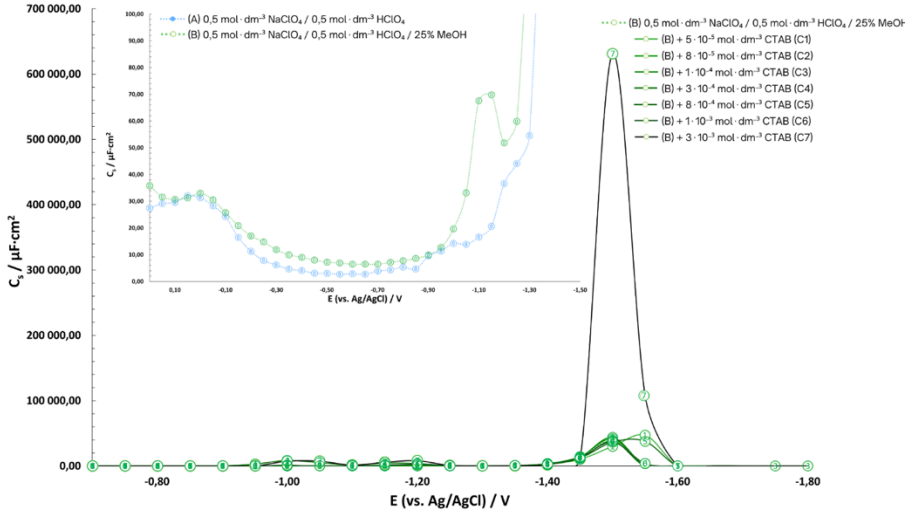

Fig. 2. Differential capacitance curves for system B: 0.5 mol·dm^{-3} $NaClO_4$ + 0.5 mol·dm^{-3} $HClO_4$ /25%$_{(v/v)}$ MeOH and in the presence of CTAB (5.0·10^{-5}-3.0·10^{-3} mol·dm^{-3})

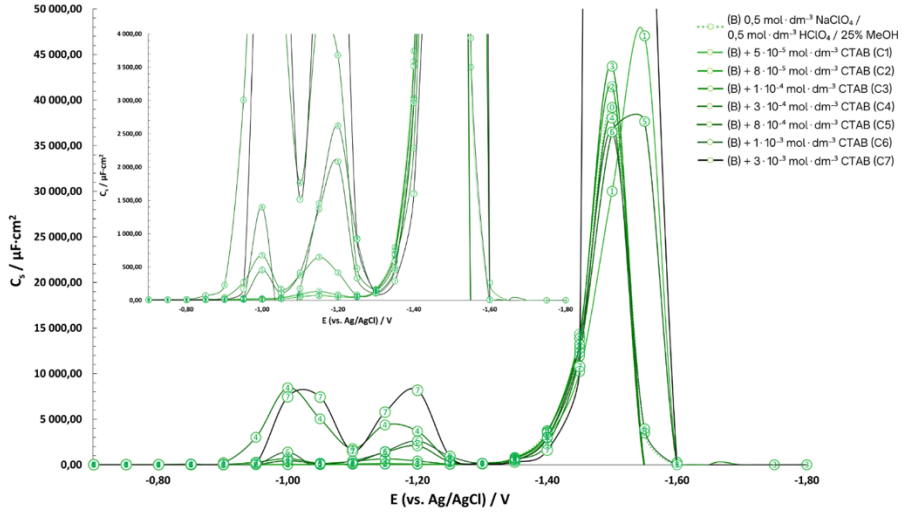

Fig. 3. Differential capacitance curves for system B: 0.5 mol·dm^{-3} $NaClO_4$ + 0.5 mol·dm^{-3} $HClO_4$ /25%$_{(v/v)}$ MeOH and in the presence of CTAB (5.0·10^{-5}-3.0·10^{-3} mol·dm^{-3})

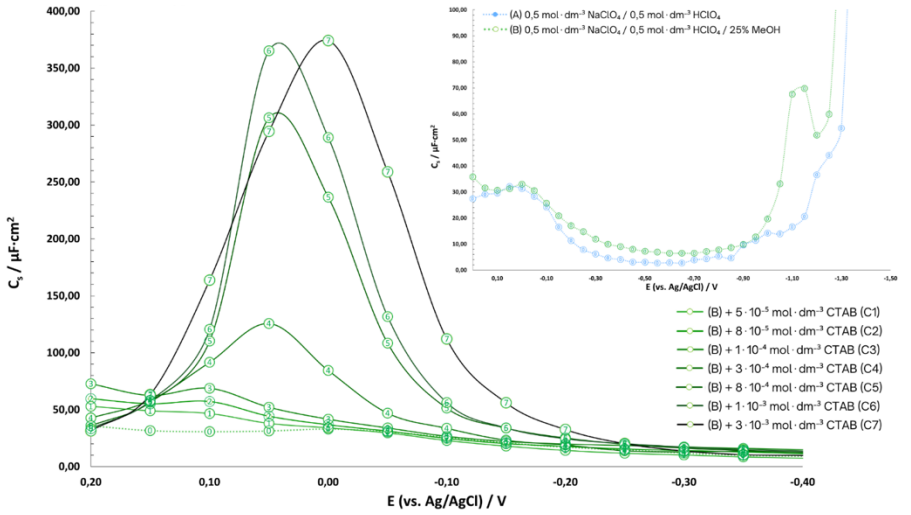

Fig. 4. Differential capacitance curves for system B: 0.5 mol·dm^{-3} $NaClO_4$ + 0.5 mol·dm^{-3} $HClO_4$ /25%$_{(v/v)}$ MeOH and in the presence of CTAB (5.0·10^{-5}-3.0·10^{-3} mol·dm^{-3})

capacitance (around -0.05 V and -1.1 V) and a distinct decrease (near -0.4 V) are also observed from a CTAB concentration of $8 \cdot 10^{-4}$ mol·dm^{-3} onwards. This concentration, determined experimentally in the present study, corresponds to the critical micelle concentration (CMC), identifying the formation of hemimicelles or micelles. The possibility of synergistic interactions between these molecular species cannot be ruled out.

The differential capacitance curves obtained for system D, containing 25%$_{(v/v)}$ ethanol and increasing concentrations of CTAB (Figs. 7–8), exhibit characteristic adsorption peaks in the positive potential range (~0.0-0.15 V) (Fig. 7). In comparison with the methanolic systems, where a distinct adsorption peak of the alcohol itself was observed (Fig. 5), in the presence of ethanol this feature is only weakly pronounced (around -0.4 V). This indicates a weaker contribution of ethanol to the establishment of the adsorption equilibrium. With increasing surfactant concentration, the peak heights systematically increase, and their potentials shift slightly towards more negative values. This behaviour most likely reflects competitive adsorption between ethanol and CTAB within the adsorbed layer, with CTAB clearly predominating in the interfacial adsorption process (Gisbert-González et al., 2023; Knag, Sjöblom, Gulbrandsen, 2005).

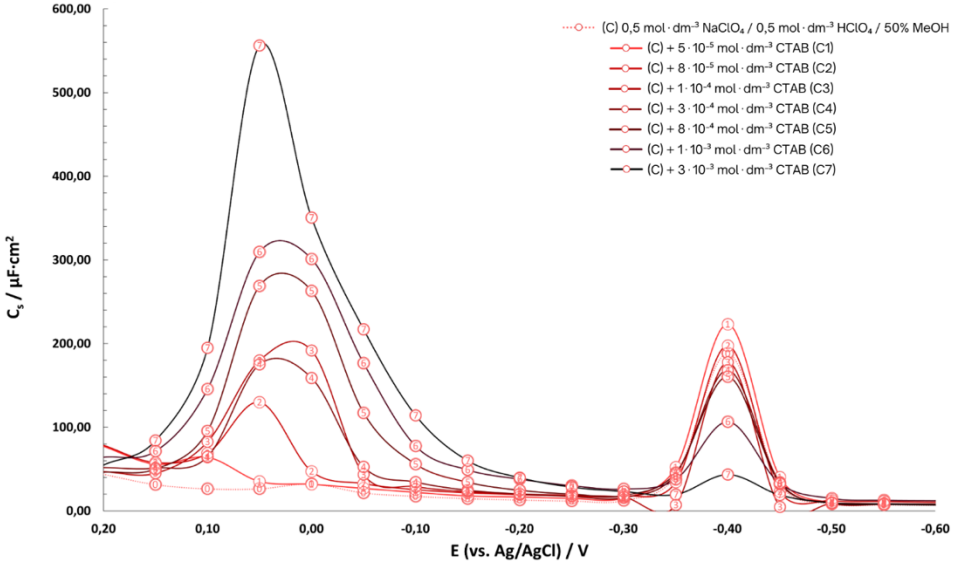

Fig. 5. Differential capacitance curves for system C: 0.5 mol·dm^{-3} $NaClO_4$ + 0.5 mol·dm^{-3} $HClO_4$ /50%$_{(v/v)}$ MeOH and in the presence of CTAB ($5.0 \cdot 10^{-5}$-$3.0 \cdot 10^{-3}$ mol·dm^{-3})

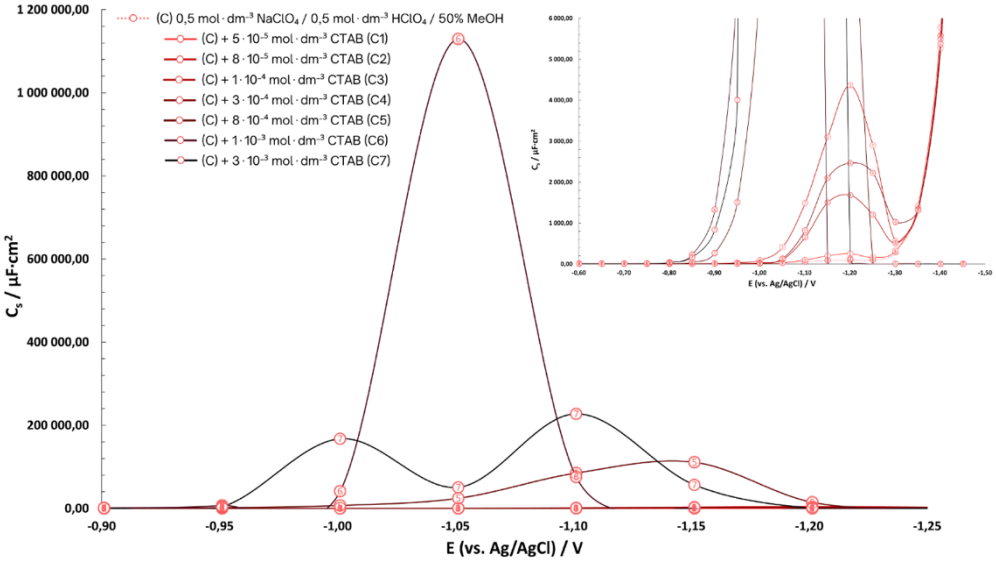

Fig. 6. Differential capacitance curves for system C: 0.5 mol·dm^{-3} $NaClO_4$ + 0.5 mol·dm^{-3} $HClO_4$ /50%$_{(v/v)}$ MeOH and in the presence of CTAB ($5.0 \cdot 10^{-5}$-$3.0 \cdot 10^{-3}$ mol·dm^{-3})

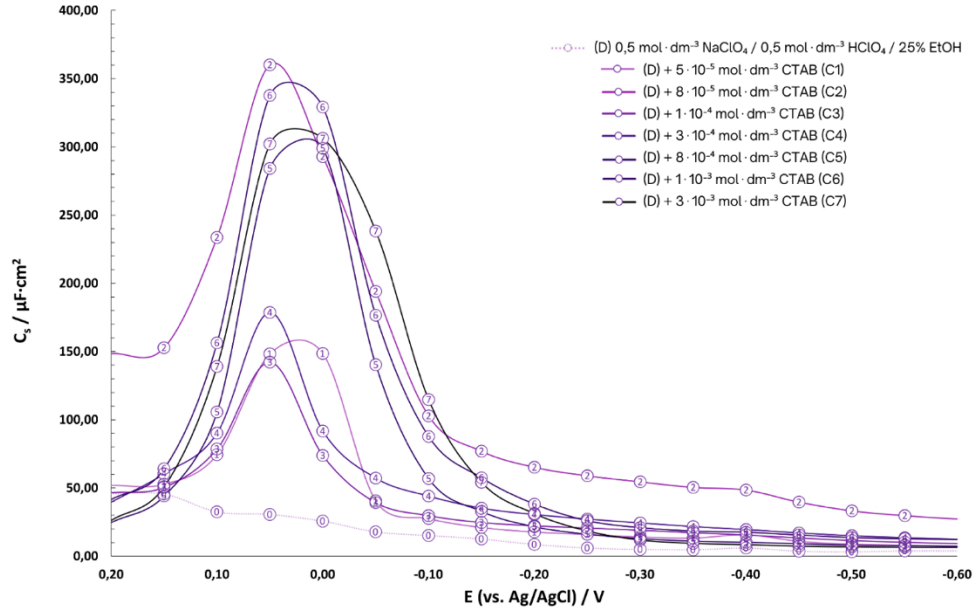

Fig. 7. Differential capacitance curves for system D: 0.5 mol·dm^{-3} $NaClO_4$ + 0.5 mol·dm^{-3} $HClO_4$ /25%$_{(v/v)}$ EtOH and in the presence of CTAB (5.0·10^{-5}-3.0·10^{-3} mol·dm^{-3})

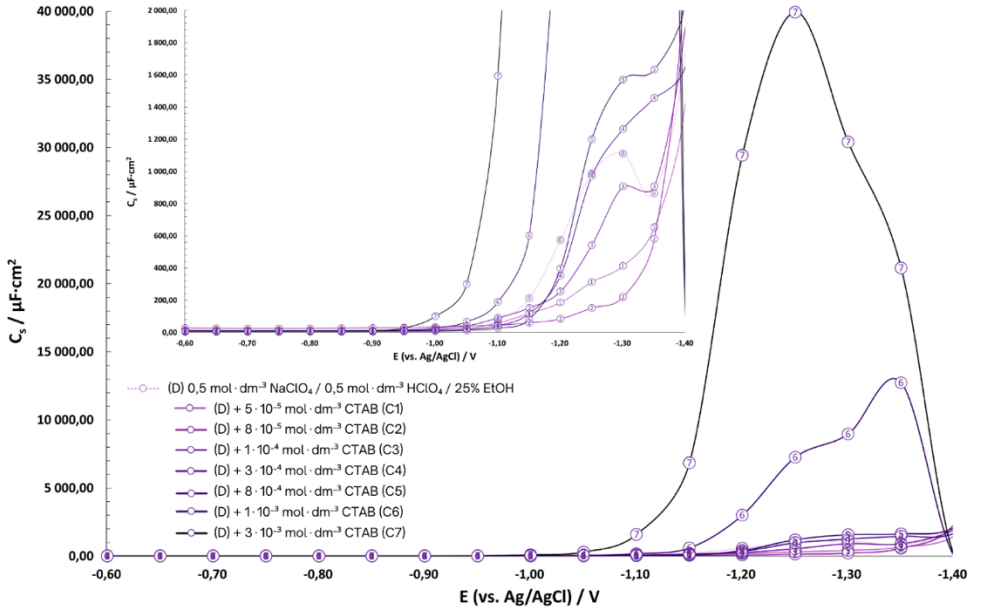

Fig. 8. Differential capacitance curves for system D: 0.5 mol·dm^{-3} $NaClO_4$ + 0.5 mol·dm^{-3} $HClO_4$ /25%$_{(v/v)}$ EtOH and in the presence of CTAB (5.0·10^{-5}-3.0·10^{-3} mol·dm^{-3})

In the negative potential range (-0.95 to -1.4 V), the differential capacitance curves obtained for the system containing 25% $_{(v/v)}$ ethanol (Fig. 8) display markedly different behaviour compared with those for methanolic solutions. The desorption peaks are poorly defined, noticeably broadened, and significantly lower in intensity than those observed for systems B and C, a difference particularly evident at the highest CTAB concentrations. In the presence of methanol, an increase in surfactant concentration leads to a systematic increase in the desorption peak height. In contrast, in the presence of ethanol, these changes are more subdued and do not reach such high values. It is noteworthy that the desorption peak initially decreases for the two lowest concentrations of CTAB. This most likely indicates hindered organisation of the adsorbed layer in the presence of ethanol. Only from approximately the fourth CTAB concentration (≥ 3·10^{-4} mol·dm^{-3}) does the peak begin to rise again, eventually exceeding the value recorded for the basic electrolyte solution without the surfactant. This behaviour suggests that

ethanol initially competes strongly with CTAB for adsorption sites, thereby destabilising the interfacial layer. However, at higher surfactant concentrations, CTAB assumes a dominant role, enabling the formation of mixed adsorbed structures (Gisbert-González et al., 2023; Wall & Zukoski, 1999).

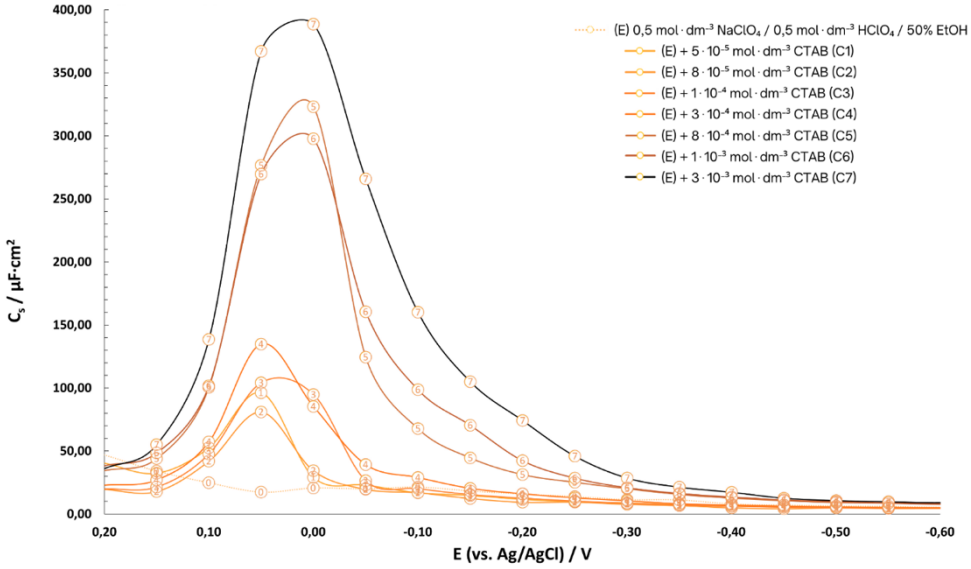

Fig. 9. Differential capacitance curves for system E: 0.5 mol·dm^{-3} $NaClO_4$ + 0.5 mol·dm^{-3} $HClO_4$ /50%$_{(v/v)}$ EtOH and in the presence of CTAB (5.0·10^{-5}-3.0·10^{-3} mol·dm^{-3})

In the system containing 50% ethanol (E) (Fig. 9), no distinct alcohol adsorption peak (~–0.40 V) is observed. CTAB predominantly shapes the adsorbed layer in this case. The surfactant adsorption peak increases with concentration, though in a non-linear manner. At lower concentrations (5·10^{-5} - 1·10^{-4} mol·dm^{-3}), the peak height increases moderately, while above 3·10^{-4} mol·dm^{-3} a pronounced enhancement is observed, indicative of layer densification and the onset of surface aggregation (CMC ≈ 5·10^{-4} mol·dm^{-3}). The peak maximum shifts towards more negative potentials (~+0.10 → -0.05 V), and its width initially decreases (signifying ordering) before broadening again at the highest concentration, suggesting the formation of hemimicellar or mixed CTAB-alcohol micelle structures (Bielawska et al., 2013). Compared to the methanolic systems, the peaks appear cleaner (with negligible alcohol contribution) and the growth dynamics are less abrupt, indicating that, at high ethanol content, the dominant role of CTAB in the adsorbed layer is again evident.

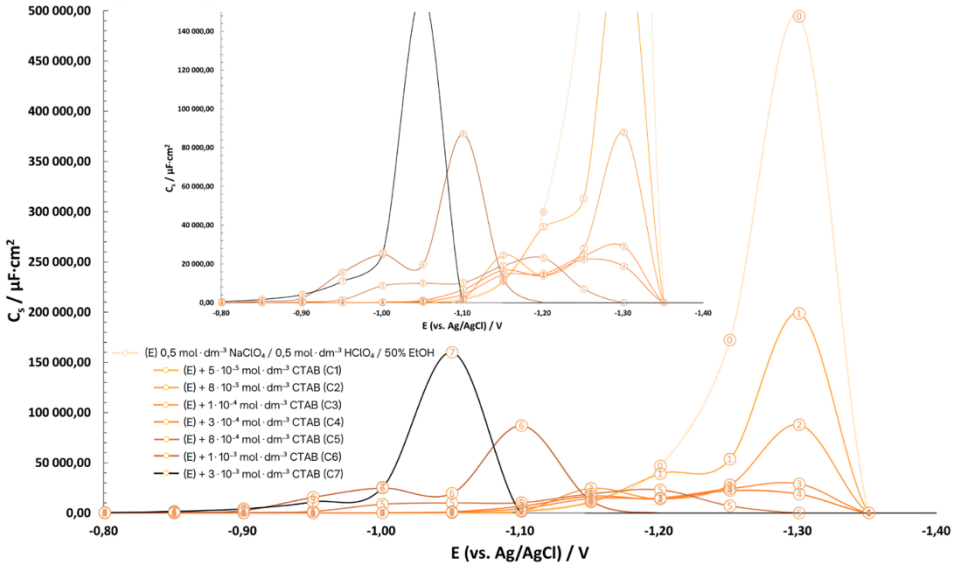

Fig. 10. Differential capacitance curves for system E: 0.5 mol·dm^{-3} $NaClO_4$ + 0.5 mol·dm^{-3} $HClO_4$ /50%$_{(v/v)}$ EtOH and in the presence of CTAB (5.0·10^{-5}-3.0·10^{-3} mol·dm^{-3})

In the negative potential range for system E (Fig. 10), the differential capacitance curves exhibit a complex desorption pattern that differs significantly from the previous systems (A–D). The desorption peak of the blank (0) is the highest and narrowest, indicating facile and homogeneous desorption of the solvent layer and the basic electrolyte ions. Upon addition of CTAB, the C1 peak remains relatively high. Still, from C2 to C5, the peak maximum systematically decreases, the curves become poorly defined, and the peak position shifts towards more positive potentials (for C5, the lowest signal and the most pronounced shift are observed). This behaviour indicates that at low and moderate CTAB concentrations, the surfactant displaces solvent molecules and binds more strongly to the amalgam electrode surface, most likely leading to a more disordered desorption mechanism and the formation of an adsorbed layer with heterogeneous structure. Only above the micelle formation threshold (CMC ≈ $8{\cdot}10^{-4}$ mol·dm^{-3}), i.e., for C6 and C7, a sharp increase in desorption peak height is observed, accompanied by a further shift of the peak maxima towards more positive potentials. In this range, the signal corresponds to the desorption of surface aggregates (hemimicelles/micelles), which cooperatively detach from the electrode, reflecting a transition toward more thermodynamically stable structures that form to minimise the system's free energy (Rosen, Kunjappu, 2012). It can therefore be concluded that, in the presence of ethanol, CTAB forms looser, more aggregated surface layers, in which solvent competition weakens hydrophobic interactions and promotes reorganisation into less-ordered interfacial structures (Bielawska et al., 2013).

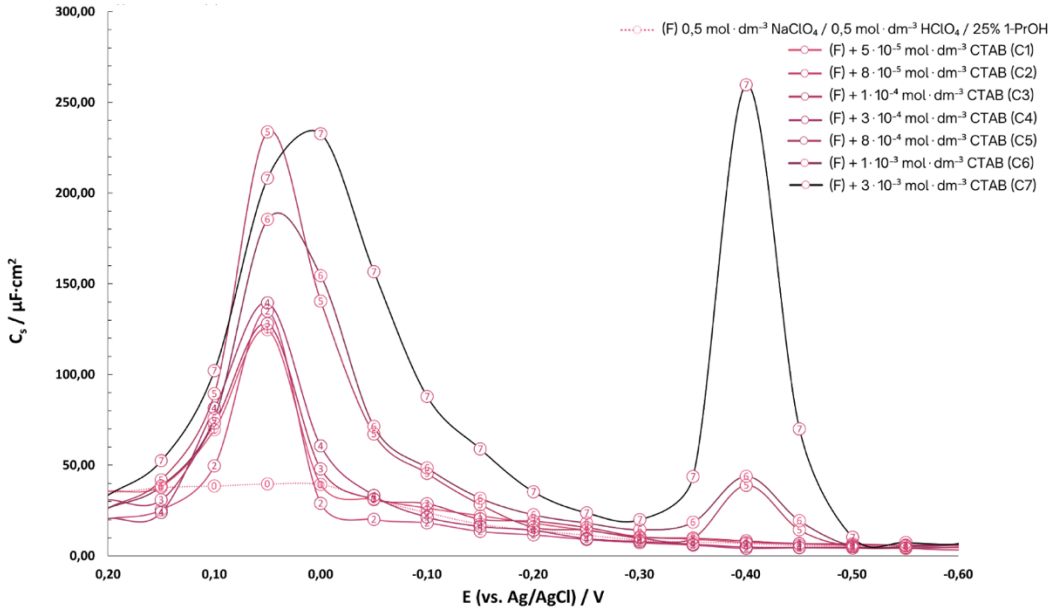

Fig. 11. Differential capacitance curves for system F: 0.5 mol·dm^{-3} $NaClO_4$ + 0.5 mol·dm^{-3} $HClO_4$ /25%$_{(v/v)}$ 1-PrOH and in the presence of CTAB ($5.0{\cdot}10^{-5}$-$3.0{\cdot}10^{-3}$ mol·dm^{-3})

In the more positive potential region, the differential capacitance curves for system F (25%$_{(v/v)}$ 1-PrOH) (Fig. 11) differ markedly from those obtained for the methanolic and ethanolic systems. No distinct alcohol adsorption peak (~-0.40 V), characteristic of methanol, is observed, nor even its weak outline noted in the ethanolic system: the adsorbed layer in this case is shaped almost exclusively by CTAB. The main CTAB adsorption peak increases with surfactant concentration, exhibiting moderate growth at lower concentrations (C1-C4), while a pronounced enhancement of the signal occurs from C5 onwards. The peak maximum gradually shifts towards more negative potentials (from approximately +0.10 V to around 0 V to -0.05 V). At higher CTAB concentrations (C5-C7), a second peak appears at approximately -0.40 V. Its occurrence, dependent on CTAB concentration, does not correspond to the "pure" alcohol adsorption observed in the methanolic or ethanolic systems, but rather indicates a cooperative reorganisation of the surfactant adsorption layer and the onset of hemimicelle formation, most likely accompanied by displacement of 1-PrOH molecules from the interfacial region (Bielawska et al., 2013, Wall, Zukoski, 1999). The width of the central peak initially decreases (reflecting layer ordering) and subsequently increases again for C7, confirming a transition from adsorption of

individual CTAB monomers to surface aggregation processes. Compared with systems B-E, system F, containing 1-PrOH, exhibits lower and broader peaks, indicative of weakened adsorption dynamics and, most likely, stronger competition between alcohol molecules and CTAB for adsorption sites on the electrode surface.

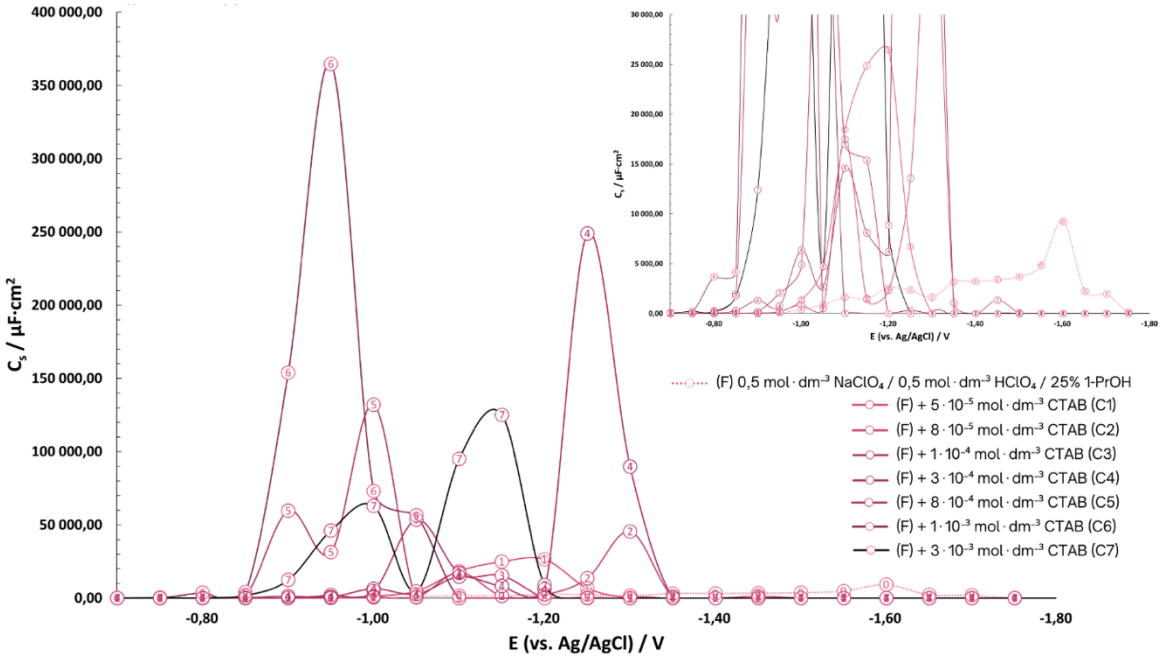

Fig. 12. Differential capacitance curves for system F: 0.5 mol·dm^{-3} $NaClO_4$ + 0.5 mol·dm^{-3} $HClO_4$ /25%$_{(v/v)}$ 1-PrOH and in the presence of CTAB (5.0·10^{-5}-3.0·10^{-3} mol·dm^{-3})

In the more negative potential region, the differential capacitance curves for system F (25%$_{(v/v)}$ 1-PrOH) (Fig. 12) display a markedly different behaviour compared with the previously studied mixed aqueous–organic systems. Even for the blank (0), the desorption signal exhibits an extended profile. Instead of a single sharp maximum, several overlapping, partially developed peaks are observed, suggesting that the mere presence of 1-PrOH induces a complex, multistep reorganisation of the adsorbed layer and likely partial cooperative interactions between alcohol molecules and other ions in solution. Upon the addition and gradual increase of CTAB concentration, the signal shape becomes even more complex and changes non-linearly. The peaks broaden, often displaying more than one maximum, and their heights are significantly lower than those observed in methanolic systems. With increasing CTAB concentration (C1-C5), a gradual flattening and splitting of the desorption peak is observed, indicating the superposition of desorption processes involving various molecular species within the mixed adsorbed layer, from CTAB monomers coordinated with alcohol molecules to loosely ordered aggregates. Only at concentrations approaching the CMC (C6-C7) does a more pronounced increase in signal intensity appear, which can be attributed to collective reorganisation and desorption of CTAB hemimicelles. However, even under these conditions, the curves remain less steep and more dispersed than those recorded for methanolic or ethanolic solutions. Overall, these findings indicate that 1-PrOH exerts the strongest disruptive influence on the desorption process, promoting a multistep release mechanism of molecules from the surface of the R-AgLAFE amalgam electrode in mixed aqueous–organic electrolyte solutions.

In system G, containing 50%$_{(v/v)}$ 1-PrOH (Fig. 13), the differential capacitance curves exhibit a distinct, well-defined adsorption peak of CTAB, whose intensity increases with rising surfactant concentration. The peak maximum shifts towards more negative potentials (from approximately +0.05 V to around 0 V), while its width decreases. Compared with the methanolic and ethanolic systems, the curves display a more regular profile, without additional peak features in the region of -0.40 V, suggesting a reduced contribution of the alcohol to the formation of the adsorbed layer. The adsorption of CTAB clearly dominates, and the high concentration of 1-PrOH (50% $_{(v/v)}$) appears to stabilise the structure and the presence of specific molecular forms within the surface layer.

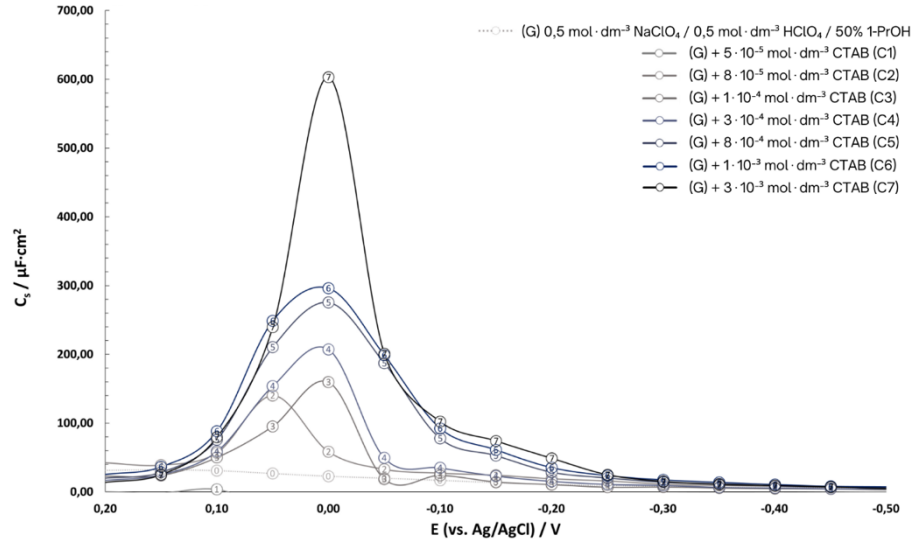

Fig. 13. Differential capacitance curves for system G: 0.5 mol·dm^{-3} $NaClO_4$ + 0.5 mol·dm^{-3} $HClO_4$ /50%$_{(v/v)}$ 1-PrOH and in the presence of CTAB (5.0·10^{-5}-3.0·10^{-3} mol·dm^{-3})

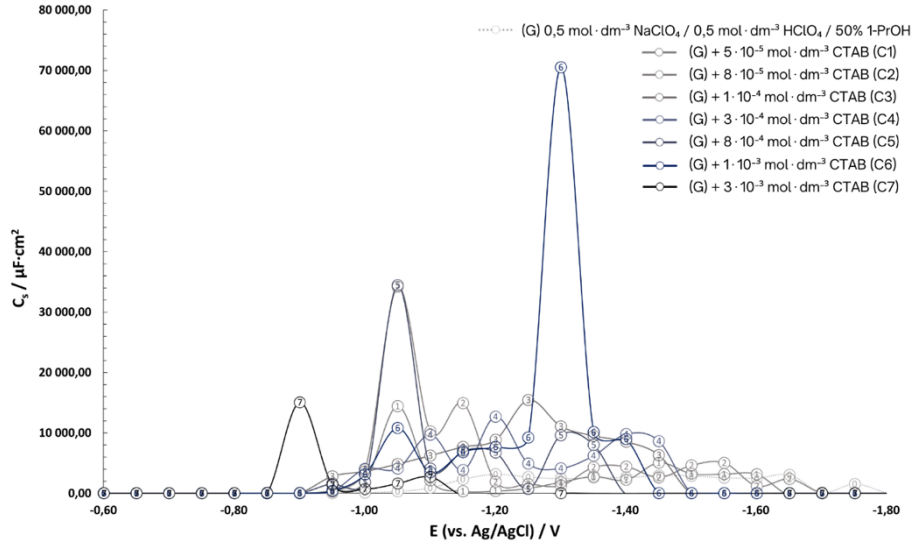

Fig. 14. Differential capacitance curves for system G: 0.5 mol·dm^{-3} $NaClO_4$ + 0.5 mol·dm^{-3} $HClO_4$ /50%$_{(v/v)}$ 1-PrOH and in the presence of CTAB (5.0·10^{-5}-3.0·10^{-3} mol·dm^{-3})

In the negative potential range, the differential capacitance curves for system G (Fig. 14) exhibit a multistep, non-linear desorption behaviour. The desorption peak of the blank (0) is low and broad, with several minor maxima, reflecting solvent desorption. Upon the addition of CTAB, even at the lowest concentration (C1), a distinct, sharp signal appears around -1.05 V, accompanied by additional, smaller peaks at more negative potentials. For subsequent concentrations (C2-C4), a pronounced signal splitting is observed: instead of a single desorption peak, groups of partially overlapping and irregular maxima emerge, differing in both intensity and position. This pattern suggests a multistage desorption process involving various structural forms of CTAB, from individual molecules to surface aggregates stabilised by the presence of alcohol. Only from C5 onward do the profiles become partially ordered; at C6 and C7, a dominant, tall, and relatively narrow peak appears, though smaller maxima still accompany it. This indicates the coexistence of multiple structures within the adsorbed/desorbed layer, including hemimicelles, loosely packed aggregates, and dense CTAB domains, each desorbing at different energies (Zhang, Somasundaran, 2006; Paria, 2004). The high 1-PrOH content appears to enhance further these instabilities: screening of the cationic headgroups and reduced hydrophobic interactions result in a multistep, strongly nonlinear, and inherently unpredictable desorption sequence.

3.2. Determination of zero charge potential and surface tension

The values of the zero-charge potential (E_z) and the corresponding surface tension (γ_z) are summarised in Tables 1–3 for the mixed chlorate(VII)/alcohol systems, both in the absence and in the presence of CTAB.

Table 1. The values of the zero-charge potential (E_z) and the corresponding surface tension (γ_z) for the mixed aqueous–methanolic SEs, both in the absence and in the presence of CTAB

C_{CTAB} [mol·dm^{-3}]	C_{MeOH} [%]					
	0		25		50	
	E_z [mV]	γ_z [mNm^{-1}]	E_z [mV]	γ_z [mNm^{-1}]	E_z [mV]	γ_z [mNm^{-1}]
0	-435.9	451.7	-384.6	436.2	-276.4	432.7
5·10^{-5}	-448.0	449.1	-397.1	432.7	-268.6	430.1
8·10^{-5}	-440.4	447.3	-391.4	431.6	-298.4	426.0
1·10^{-4}	-435.6	448.2	-388.9	431.9	-335.8	422.4
3·10^{-4}	-425.1	435.7	-377.3	427.8	-304.9	422.8
8·10^{-4}	-366.5	425.2	-367.2	426.2	-312.0	419.7
1·10^{-3}	412.1	424.1	-364.6	425.0	-304.6	420.7
3·10^{-3}	-399.3	415.8	-353.1	420.6	-317.4	418.2

Table 2. The values of the zero-charge potential (E_z) and the corresponding surface tension (γ_z) for the mixed aqueous–ethanolic SEs, both in the absence and in the presence of CTAB

C_{CTAB} [mol·dm^{-3}]	C_{EtOH} [%]					
	0		25		50	
	E_z [mV]	γ_z [mNm^{-1}]	E_z [mV]	γ_z [mNm^{-1}]	E_z [mV]	γ_z [mNm^{-1}]
0	-435.9	451.7	-297.2	424.1	-245.6	409.5
5·10^{-5}	-448.0	449.1	-315.3	423.2	-225.7	411.2
8·10^{-5}	-440.4	447.3	-304.6	423.1	-226.1	410.9
1·10^{-4}	-435.6	448.2	-295.6	422.4	-226.4	409.5
3·10^{-4}	-425.1	435.7	-292.0	417.6	-228.8	409.7
8·10^{-4}	-366.5	425.2	-288.3	405.7	-230.5	410.5
1·10^{-3}	412.1	424.1	-286.4	399.1	-232.2	412.0
3·10^{-3}	-399.3	415.8	-272.3	390.8	-219.9	413.5

Table 3. The values of the zero-charge potential (E_z) and the corresponding surface tension (γ_z) for the mixed aqueous–1-propanolic SEs, both in the absence and in the presence of CTAB

C_{CTAB} [mol·dm^{-3}]	$C_{1\text{-}PrOH}$ [%]					
	0		25		50	
	E_z [mV]	γ_z [mNm^{-1}]	E_z [mV]	γ_z [mNm^{-1}]	E_z [mV]	γ_z [mNm^{-1}]
0	-435.9	451.7	-257.0	441.3	-239.5	432.3
5·10^{-5}	-448.0	449.1	-248.4	443.9	-247.5	430.1
8·10^{-5}	-440.4	447.3	-255.0	442.2	-244.1	431.9
1·10^{-4}	-435.6	448.2	-264.5	438.8	-239.8	433.6
3·10^{-4}	-425.1	435.7	-278.3	437.9	-245	431.9
8·10^{-4}	-366.5	425.2	-279.3	435.3	-252.1	428.4
1·10^{-3}	412.1	424.1	-306.4	434.4	-236.8	434.5
3·10^{-3}	-399.3	415.8	-281.6	432.7	-95.3	455.1

It was observed that the addition of alcohols causes a shift of E_z towards more positive potentials, accompanied by a decrease in γ_z (Ehrlich, Ehrlich, Jänes & Lust, 1999). Such changes suggest that alcohol and surfactant molecules interact with the electrode surface, altering the local charge distribution within the mixed adsorbed layer. These observations may reflect different orientations of alcohol molecules at the R-AgLAFE electrode/solution interface, particularly in the case of ethanol and 1-propanol. According to the concept proposed by Frumkin (1925) and Parsons (1969), a positive shift in E_z indicates the presence of positively charged surfactant species in the near-electrode layer, while a reduction in γ_z is associated with the adsorption of organic molecules and a decrease in surface energy. Similar adsorption effects have been previously reported (Nosal-Wiercińska, 2010; Damaskin, B., Kazarinov, V.E., 1980). The obtained relationships between the zero-charge potential and the surface tension are consistent with the trends observed in the differential capacitance curves, confirming that complex and competitive adsorption processes occur at the R-AgLAFE/solution interface.

4. Conclusions

The results provide experimental evidence for the coexistence of competitive and cooperative effects in the adsorption of surfactants and alcohols, phenomena rarely examined by electrochemical methods. Simultaneous analysis of changes in differential capacitance, zero-charge potential (E_z), and surface tension (γ_z) revealed the dynamic nature of adsorption at the R-AgLAFE/solution interface. This indicates that the adsorption equilibrium is not maintained. The observed relationships demonstrate competitive interactions between ions present in the solutions, which influence the variable structure of the mixed adsorbed layer. Alcohols act as co-modifiers of the interfacial region, affecting both the local dielectric properties and the mode of CTAB adsorption. Depending on the alcohol's carbon chain length, different effects on adsorption equilibrium were observed: methanol generally maintains equilibrium, whereas ethanol and 1-propanol destabilise it. These findings fill an existing research gap, showing that for the R-AgLAFE silver amalgam electrode, the co-adsorption of cationic surfactants and low-molecular-weight alcohols results in structurally heterogeneous adsorbed layers whose organisation is difficult to predict and control under the experimental conditions used.

References

BARD, A.J., FAULKNER, L.R., WHITE, H.S., 2022. *Electrochemical Methods: Fundamentals and Applications*, 3rd ed. Wiley, Hoboken, NJ.

BHATTARAI, A., 2015. *Studies of the micellization of cationic–anionic surfactant systems in water and methanol–water mixed solvents*. Journal of Solution Chemistry, 44, 2090–2105.

BIELAWSKA, M., CHODZIŃSKA, A., JAŃCZUK, B., ZDZIENNICKA, A., 2013. *Determination of CTAB CMC in mixed water + short-chain alcohol solvent by surface tension, conductivity, density and viscosity measurements*. Colloids Surf. A Physicochem. Eng. Asp., 424, 81–88.

BREITER, M.W., 1962. *Double layer capacity and methanol coverage on platinum in perchloric acid solution*. Electrochimica Acta 7(5), 533–542.

CHIBOWSKI, S., WIŚNIEWSKA, M., 2021. *Wpływ surfaktantów na właściwości adsorpcyjne substancji organicznych i jonów metali ciężkich w układach koloidalnych*. Wiadomości Chemiczne 75(9–10), art. 10.

DAMASKIN, B.B., KAZARINOV, V.E., 1980. T*he Adsorption of Organic Molecules*. In: BOCKRIS, J.O., CONWAY, B.E., YEAGER, E. (eds) Comprehensive Treatise of Electrochemistry. Springer, Boston, MA.

EHRLICH, J., EHRLICH, T., JÄNES, A., LUST, E., 1999. *The zero charge potential shift upon adsorption of various organic compounds at bismuth|solution interface*. Electrochimica Acta, 45(6), 935–943.

FIC, K., LOTA, G., FRĄCKOWIAK, E., 2012. *Effect of surfactants on capacitance properties of carbon electrodes*. Electrochimica Acta 60, 206–212.

GISBERT-GONZÁLEZ, J.M., RÓDENAS-RIBES, J., CABANES-GALLEGO, F., GARCÍA-JAREÑO, J.J., VICENTE, F., 2023. *Spectroelectrochemical studies of CTAB adsorbed on gold electrodes*. Langmuir, 39, 7, 2761–2770.

GU, S., HAOYI, Y., YUAN, Y., GAO, Y., ZHU, N., WU, F., BAI, Y., WU, C., 2022. *Solvent effects on kinetics and electrochemical performances of rechargeable aluminium batteries*. Energy Materials Advances 2022, 9790472.

GUGAŁA-FEKNER, D., NIESZPOREK, J., SIENKO, D., 2015. *Adsorption of anionic surfactant at the electrode–$NaClO_4$ solution interface*. Monatshefte für Chemie – Chemical Monthly 146, 541–545.

IWASAKI, H., KIMURA, Y., UEMATSU, Y., 2023. *Ubiquitous preferential water adsorption to electrodes in water/1-propanol mixtures detected by electrochemical impedance spectroscopy*. Journal of Physical Chemistry C 127(48), 23382–23389.

JIA, Y.F., THOMAS, K.M., 2000. *Adsorption of cadmium ions on oxygen surface sites in activated carbon*. Langmuir 16, 1114–1122.

KISS, L., SZABÓ, P., KUNSÁGI-MÁTÉ, S., 2025. *Electrochemical Polymerization of Guaiacol in Organic Solvents and Analytical Performance of the Poly(Guaiacol) Modified Electrode Towards Phenol Antioxidants*. Chemosensors 13(6), 214.

KNAG, M., SJÖBLOM, J., GULBRANDSEN, E., 2005. *The effect of straight chain alcohols and ethylene glycol on the adsorption of CTAB on gold.* J. Dispersion Sci. Technol., 26, 207–217.

KUSU, F., TAKAMURA, K., WATANABE, M., 1993. *Specular reflection studies on the adsorption of quaternary ammonium ions at a glassy carbon electrode.* Analytical Sciences 9(5), 583–589.

LASIA, A., 2014. *Electrochemical Impedance Spectroscopy and Its Applications*. Springer, New York, USA.

MARTYNA, M., NOSAL-WIERCIŃSKA, A., GOŁĘBIOWSKA, B., 2022. *Application of the nanostructured R-AgLAFE electrode for the Bi(III) electroreduction in the presence of 2-thiocytosine from chlorates(VII) with varied water activity.* Electrocatalysis 13, 425–434.

MONCELLI, M.R., FORESTI, M.L., GUIDELLI, R., 1990. *Trends in the adsorption behaviour of n-aliphatic alcohols on mercury from aqueous 0.5 M Na_2SO_4.* Journal of Electroanalytical Chemistry and Interfacial Electrochemistry 295 (1–2), 225–238.

NIESZPOREK, J., 2013. *Adsorption of tert-butanol at the electrode from concentrated $NaClO_4$ solutions*. Open Chemistry 11(1), 86–93.

NIESZPOREK, J., 2020. *Nicotinamide as a Catalyst for Zn^{2+} Electroreduction in Acetate Buffer*. Electrocatalysis 11, 422–431.

NOSAL-WIERCIŃSKA, A., MARTYNA, M., GROCHOWSKI, M. & BAŚ, B., 2021. *First electrochemical studies on "CAP–PAIR" effect for Bi(III) ion electroreduction in the presence of 2-thiocytosine on novel cyclically renewable liquid silver amalgam film electrode (R-AgLAFE).* Journal of The Electrochemical Society, 168(6), 066504.

NOSAL-WIERCIŃSKA, A., DALMATA, G., 2010, *Adsorption of Methonine at Mercury/Aqueous Solution of Chlorate(VII) Interface; Dependence on the Supporting Electrolyte Concentration*. Electroanalysis, 22: 2081-2086.

PAJKOSSY, T., 2005. *Impedance spectroscopy at interfaces of metals and aqueous solutions - Surface roughness, CPE and related issues*. Solid State Ionics 176, 1997–2003.

PARIA, S., 2004. *A review on experimental studies of surfactant adsorption at the hydrophilic solid–water interface*. Adv. Colloid Interface Sci. 110(3), 75–95.

PIKMA, P., ERS, H., SIINOR, L. et al., 2023. *The review of advances in interfacial electrochemistry in Estonia: electrochemical double layer and adsorption studies for the development of electrochemical devices*. J. Solid State Electrochem. 27, 1547–1591.

ROSEN, M.J., KUNJAPPU, J.T., 2012. *Micelle Formation by Surfactants. In: Surfactants and Interfacial Phenomena*, 4th ed. Wiley, Hoboken, NJ.

SATHYANARAYANA, S., 1974. *Mechanism of adsorption effects on electrode kinetics: Part I. Selection rules in the case of low coverage by molecular surfactants*. J. Electroanal. Chem. Interfacial Electrochem. 50, 195–209.

SAWAMOTO, H., 2003. *Reversible and irreversible adsorption of surfactants at a hanging mercury drop electrode*. Analytical Sciences 19, 1381–1386.

SCHIFFRIN, D.J., 1969. *Interfacial tension measurements between mercury and dilute aqueous electrolytes*. Journal of Electroanalytical Chemistry and Interfacial Electrochemistry, 23(1), 168–171.

SYKUT, K., DALMATA, G., NOWICKA, B., SABA, J., 1978. *Acceleration of electrode processes by organic compounds - "cap-pair"* effect. Journal of Electroanalytical Chemistry and Interfacial Electrochemistry 90(2), 299–302.

ŠVANCARA, I., SÝS, M., 2023. *Carbon paste electrodes surface-modified with surfactants: principles of surface interactions at the interface between two immiscible liquid phases*. Sensors 23 (24), 9891.

WALL, J.F., ZUKOSKI, C.F., 1999. *Alcohol-induced structural transformations of surfactant aggregates*. Langmuir, 15(22), 7432–7437.

YÁÑEZ, C., GUTIÉRREZ, C., URETA-ZAÑARTU, M.S., 2003. *Electrooxidation of primary alcohols on smooth and electrodeposited platinum in acidic solution*. J. Electroanal. Chem., 541, 39–49.

ZHANG, J., MENG, Y., TIAN, Y., ZHANG, X., 2015. *Effect of concentration and addition of ions on the adsorption of sodium dodecyl sulfate on stainless steel surface in aqueous solutions*. Colloids and Surfaces A: Physicochemical and Engineering Aspects 484, 408–415.

ZHAO, L., PENG, Y., DOU, P., LI, Y., HE, T., RAN, F., 2024. *Surface chemistry of electrode materials toward improving electrolyte-wettability: A method review*. InfoMat 6 (11), e12597.

ZHANG, R., SOMASUNDARAN, P., 2006. *Advances in adsorption of surfactants and their mixtures at solid/solution interfaces.* Adv. Colloid Interface Sci. 123–126, 213–229.